CAAI Transactions on Intelligence Technology 2 (2017) 12–25

Contents lists available at ScienceDirect

CAAI Transactions on Intelligence Technology

journal homepage: http://www.journals.elsevier.com/caai-transactions-on-intelligence-technology/

Original article

A hybrid stochastic fractal search and pattern search technique based cascade PI-PD controller for automatic generation control of multi-source power systems in presence of plug in electric vehicles

Sasmita Padhy, Sidhartha Panda*

Department of Electrical Engineering, VSSUT, Burla, 768018, Odisha, India

ARTICLE INFO

Article history:
Received 4 November 2016
Received in revised form
11 January 2017
Accepted 25 January 2017
Available online 2 February 2017

Keywords:
Automatic generation control
Cascade PI-PD controller
Stochastic fractal search
Pattern search
Plug in electric vehicles

ABSTRACT

A hybrid Stochastic Fractal Search plus Pattern Search (hSFS-PS) based cascade PI-PD controller is suggested in this paper for Automatic Generation Control (AGC) of thermal, hydro and gas power unit based power systems in presence of Plug in Electric Vehicles (PEV). Firstly, a single area multi-source power system consisting of thermal hydro and gas power plants is considered and parameters of Integral (I) controller is optimized by Stochastic Fractal Search (SFS) algorithm. The superiority of SFS algorithm over some recently proposed approaches such as optimal control, differential evolution and teaching learning based optimization techniques is demonstrated by comparing simulation results for the identical power system. To improve the system performance further, Pattern Search (PS) is subsequently employed. The study is further extended for different controllers like PI, PID, and cascaded PI-PD controller and the superiority of cascade PI-PD controller over conventional controllers is demonstrated. Then, cascade PI-PD controller parameters of AGC searched using the proposed hSFS-PS algorithm in presence of plug in electric vehicles. The study is also extended to an interconnected power system. It is seen from the comparative analysis that hSFS-PS tuned PI-PD controller in single and multi-area with multi sources improves the system frequency stability in complicated situations. Lastly, a three area interconnected system with PEVs with dissimilar cascade PI-PD controller in each area is considered and proposed hSFS-PS algorithm is used to tune the controller parameters in presence of nonlinearities like rate constraint of units, dead zone of governor and communication delay.

1. Introduction

For stable and reliable operation of power systems, Automatic Generation Control (AGC) is necessary. AGC maintains balance between load and generation and hence minimizes frequency errors [1,2]. In present day interconnected power system, the generation is usually made up of a combination of thermal units, hydro units as well as gas units. Gas bad units are suitable for supplying peak demands as they can be put into service quickly. When generation capacity is not sufficient to meet the increased load demand, other alternatives could be used to minimize the imbalance. Plugin Electric Vehicles (PEV) are projected to be used vigorously in the near future because of their low charging cost and less co_2 emission level [3,4]. PEVs offer an opportunity to use small distributed energy storage systems while they are plugged in Refs. [5,6]. With large numbers of PEV and the communications and sensing associated with the power grid, they could offer ancillary services for the power grid. Frequency control is an ideal capability for PEV as the duration of energy supply is short and at the same time it is the highest priced ancillary service on the market which offers greater economic returns for vehicle owners [7–10]. Thus, PEVs have potential to contribute in the AGC to preserve the system frequency as per the load variations [11].

The conceptual frameworks for actively involving highly distributed loads in power system control actions has been presented in Ref. [12] where an overview of system control objectives, including economic dispatch, automatic generation control, and spinning reserve have been provided. Reviews of existing load control programs for the provision of power system services and challenges to achieve a load control scheme which balances device-level objectives with power system-level objectives have also been

* Corresponding author.
E-mail address: panda_sidhartha@rediffmail.com (S. Panda).
Peer review under responsibility of Chongqing University of Technology.

http://dx.doi.org/10.1016/j.trit.2017.01.002

presented by the authors. Numerous control approaches have been proposed in literature for AGC of traditional interconnected systems. In this regard, Fuzzy Logic Controller (FLC) [13] and Adaptive Neuro Fuzzy Inference System (ANFIS) [14] based approaches have been proposed for AGC. However, these controllers require skilled operator for the design as well as application. Hence, these approaches are susceptible to the operator's understanding and skills. The classical Proportional Integral (PI) controller are still extensively used in industrial systems in spite of the substantial advances in recent years in modern control system as PI controllers provides satisfactory results for a variety of plants with varied operating conditions. Besides, PI controllers can be realized and are well known to engineers. For improved system performance, a PD feedback loop can be added to a PI controller to modify the poles of the plants to required locations.

Many traditional approaches pertaining to the tuning of PID controllers and its variants are available in literature [15–19]. A modified PI-PD Smith predictor has been proposed in Ref. [20] for control of processes with large time constants or an integrator or unstable plant transfer functions plus long dead-time for reference inputs and disturbance rejections. However, these methods are time consuming and optimal parameters may not be obtained. Various intelligent technique based approaches have been recently proposed for controller design [21–23]. A Genetic Algorithm (GA) based fuzzy proportional-plus-integral-proportional-plus-derivative (PI/PD) controller has been proposed in Ref. [24] for an automotive active suspension system. In Ref. [25], the distribution of Spatio-temporal interest point is organized into a salient directed graph, reflecting the salient motions aiming at adding spatio-temporal discriminant to bag-of-visual words for real-time activity recognition. Frequency control in multi-source single and multi-area power systems by optimal controller [26], Differential Evolution (DE) [27] and Teaching Learning Based Optimization (TLBO) [28] have been reported in literature.

Stochastic Fractal Search (SFS) is a recently proposed meta-heuristic algorithm motivated by the characteristics of growth using the concept of fractal [29]. SFS employs the diffusion feature that is commonly observed in random fractals, to explore the search space. The superiority of SFS over some well-known algorithms has been demonstrated in literature. However, SFS is a global optimizing technique which is intended to explore the search space. Hence, if only SFS is employed, an optimal/near-optimal solution may be obtained. Alternatively, local search techniques such as Pattern Search (PS) are intended to exploit a local area but not suitable for global optimization problems [30]. Because of their distinct strength and weakness, inspiration for the hybridization of SFS and PS arises. Therefore, a hybrid SFS and PS (hSFS-PS) based cascade PI-PD controller is suggested in this study for AGC of multi-source power systems in presence of PEVs. Initially, a single area thermal-hydro-gas units based power system is considered and SFS and hSFS-PS is used to tune the gains of conventional Integral (I) controller. The advantage of suggested hSFS-PS algorithm over SFS, DE and TLBO techniques is also established by comparative result analysis for the identical power system with identical controller. Then cascade PI-PD controller is employed and the superiority of cascade PI-PD controller over, I, PI, PID controller is demonstrated. Then, PEVs are incorporated and the effect of PEVs in AGC is accessed. Finally, the study is extended to a three area interconnected non-linear power system with PEVs with dissimilar cascade PI-PD controller in each area.

The main contributions of present work are:

- To apply a new hybrid optimization technique which takes the advantage of a recently proposed global SFS technique and local PS technique to tune the controller parameters for automatic generation control.
- To demonstrate the superiority of hybrid SFS-PS technique over similar recently proposed heuristic techniques such as DE and TLBO for the identical power system and controller.
- To verify the effectiveness of a cascade PI-PD controller compared to conventional PID controllers for AGC of power systems.
- To investigate the contribution of Plug in Electric Vehicles as an ancillary service for AGC of linear as well as nonlinear power systems.

2. System under study

At the first instance, a single area power system shown in Fig. 1 is considered. The system compromises of a hydro unit, a thermal and a gas unit. Initially integral controllers are considered for each unit. The individual generating units have their distinct regulation parameter and participation factor. According to these parameters the total load on the system is distributed among the units. The participation factors of all units should add up to unity. The details of each parameter can be found in Refs. [27,28] and also provided in Appendix A.

3. Modelling of plug in electric vehicle

Since a large number of PEVs are going to run on the road in near future, a lumped PEV model is considered in the present study. Each PEV is modeled as per its inverter capacity. The detail model of lumped PEV is provided in Fig. 2 [31] where ΔU_E is the Load Frequency Control (LFC) signal given as an input to PEV and charging/discharging power of one PEV is the output. The capacity of battery is represented by $\pm BkW$. The complex frequency is symbolized by s, the time constant of PEV is symbolized by T. The present energy of the battery is symbolized by E and controllable energy of battery is represented by limits $E_{\max}$ and $E_{\min}$. The PEV energy remains within the maximum and minimum limit of 90% and 80% of the controllable energy respectively. K_1 and K_2 are calculated as $K_1 = E - E_{\max}$, $K_2 = E - E_{\min}$, as the energy differences. The PEV do not participate in AGC when the charge is above the maximum limit ($E_{\max}$) of 90% and below the minimum limit ($E_{\min}$) of 80%. The stored energy model in Fig. 2 computes the net energy stored in the batteries in one local control center. Local control center can act as a communicating link between power grid and the electric vehicles which control several EVs.

The stored energy model of one PEV is shown in Fig. 3. At any instant of time interval t, the number of controllable EVs $N_{controllable}(t)$ which participate in AGC are calculated form information of the initial number of controllable EVs at the beginning of the interval ($N_{initial}(t)$), number of EVs moving from controllable state to driving state during that time ($N_{plugout}(t)$)) and number of EVs moving from charging state to controllable state at that time period ($N_{controlin}(t)$) as given in Eq. (1). Hence, the number of controllable EVs ($N_{controllable}(t)$) is varied as per the added number of the control in and plug out of the EVs.

$$N_{controllable}(t) = N_{initial}(t) - N_{plugout}(t) + N_{controlin}(t) \tag{1}$$

The energy expression is written as:

$$E_{control}(t) = E_{initial}(t) + E_{controlin}(t) - E_{plugout}(t) - E_{LFC}(t) \tag{2}$$

Where,$E_{initial}(t)$ is the initial energy,$E_{controlin}(t)$ is the increase in energy because of the EVs and $E_{plugout}(t)$ is the reduction in energy as a result of plug out. The increase in energy results in the change in the state of PEVs to controllable state from the charging state which is found by multiplying $N_{controlin}(t)$ by the average charging

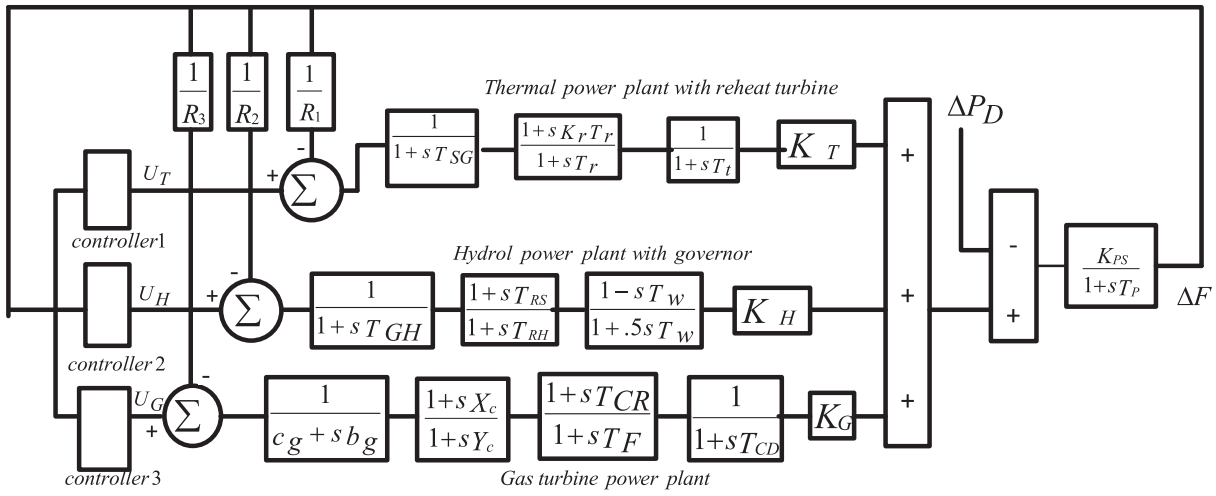

Fig. 1. Transfer function model of multi-source single area system with integral controller.

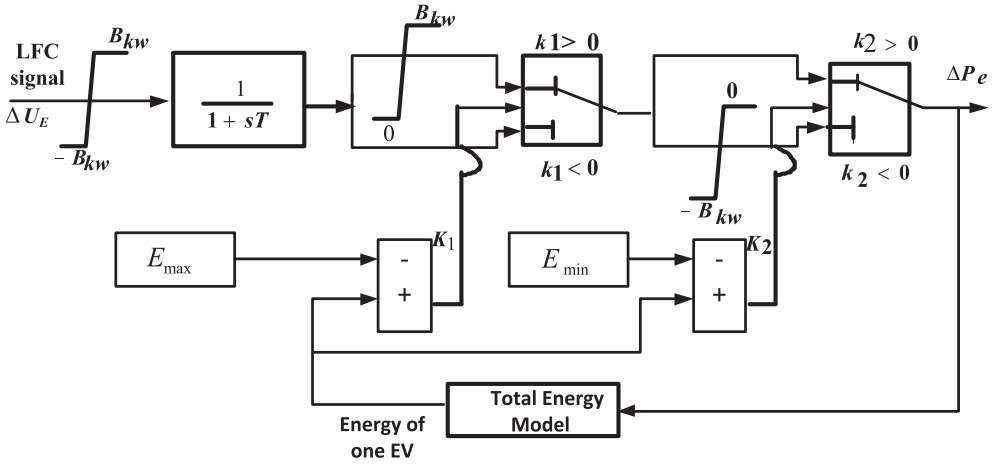

Fig. 2. Model of lumped plug in electric vehicle [31].

energy ($C^*_{kWh} = 0.8\, B^*_{kW}$). The expression for $E_{controlin}(t)$ can be written as:

$$E_{controlin}(t) = C^*_{kWh} \cdot N_{controlin}(t) = 0.8\, B^*_{kW} \cdot N_{controlin}(t) \quad [kWh] \tag{3}$$

In Fig. 3,E_{LFC} is the energy corresponding to the load frequency control signal and found by integrating local centre power (P_{LFC}).E_{LFC} can be expressed as:

$$E_{LFC}(t) = \int_0^t P_{LFC}(t)\mathrm{d}t \tag{4}$$

4. Controller structure and objective function

4.1. Controller structure

In AGC, integral based controllers are generally used to minimize the Area Control Errors (ACE) which is a linear combination of frequency & tie-line power errors and bring them back to nominal values. However, the disadvantage of using only integral controller is that it might produce a closed loop system with significantly slower response times. Proportional Integral (PI) improves the system dynamic response and also offers the additional advantages like simple design, small cost, and their usefulness when designed for systems which are linear and stable process. At the same time, conventional PI controllers are generally not efficient when the higher order nonlinear unstable systems are involved.

Cascade control is one of the approaches which can be used to improve the performance of the system. As the number of tuning nubs is more in a cascade controller than a non-cascade controller, improved system performance may be obtained. Approaches for tuning of PID controller depending on process models and cascade PI-PD controller for control systems have been proposed in literature [32–34]. Because of its improved system performance, a cascade PI-PD controller shown in Fig. 4 is chosen in the present study for AGC. The control input signals are the respective ACEs and controller output are the reference power settings of individual generating units.

4.2. Objective function

For controller design using optimization techniques, the objective function is generally specified depending on some performance criteria such as Integral of Time multiplied Absolute Error

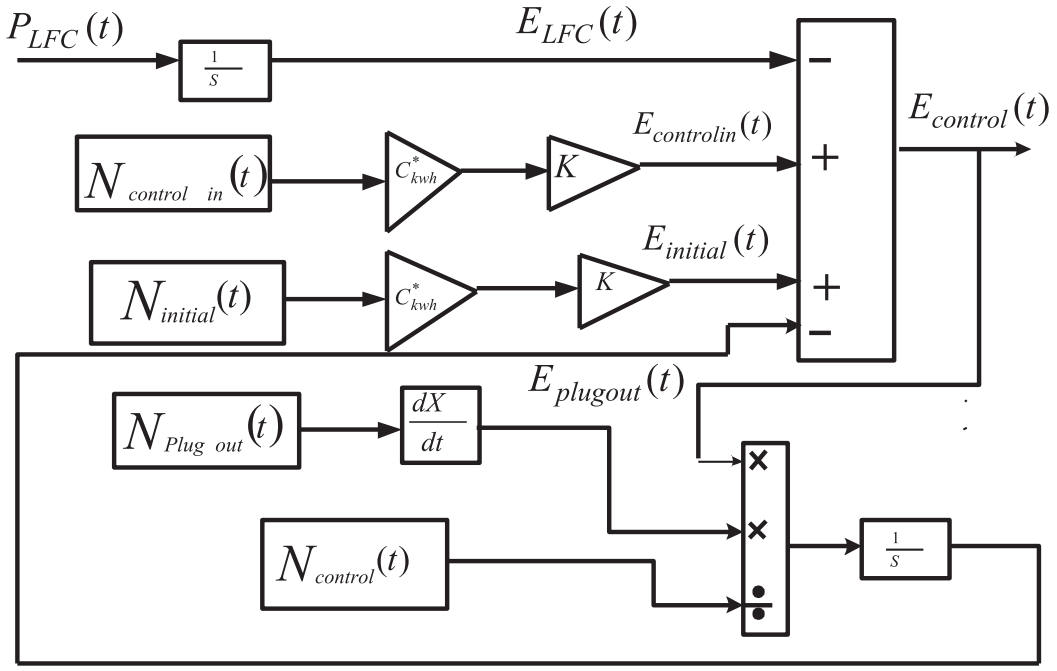

Fig. 3. Stored energy model of one local control center.

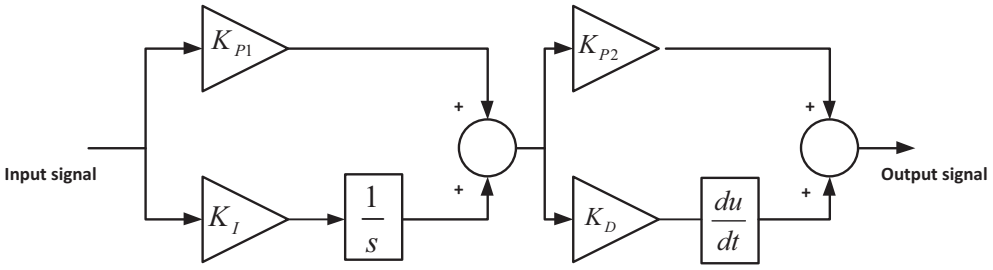

Fig. 4. Structure of cascaded PI-PD controller.

(ITAE), Integral of Squared Error (ISE), Integral of Time multiplied Squared Error (ITSE) and Integral of Absolute Error (IAE). Detailed expression of various objective functions, their comparison on the system performance are available in literature [21–23,27,28]. It has also been shown in several studies that ITAE objective function provides better system performance compared to other integral based alternatives [35,36]. Hence ITAE is chosen in the present paper as objective function which is expressed as:

$$J = ITAE = \int_0^{t_{sim}} |\Delta F|.t.dt \tag{5}$$

where, ΔF is deviation in frequency and t_{sim} is simulation time.

5. Optimization technique

5.1. Stochastic fractal search

Stochastic Fractal Search (SFS) is a recently proposed optimization algorithm motivated by the process of growth using the concept of fractal. SFS employs the diffusion characteristic that is commonly observed in fractals, to explore the search space. Stochastic rules like Gaussian walks are used to change the iteration process to generate random fractals. Given an initial particle positioned at the beginning, new particles are then created arbitrarily in random manner around that point. Diffusion process enhances the ability of algorithm to find the global minima, as well as avoids to be struck in local minima. In the next update process, the positions of points are updated in the group depending on the other points position in the group. In this process, few best particles from the diffusing process are taken, and the remaining particles are rejected. Besides well-organized examination of the search space, the algorithm uses Gaussian random approaches to update thus introducing diversification properties in SFS algorithm.

The Stochastic Fractal Search algorithm can be explained with subsequent steps [29]:

A. Initialization: Each position of particles (point) is arbitrarily initialized depending on the problem constraints by specifying lower and upper bounds as:

$$P = LB + rand(UB - LB) \tag{6}$$

Where the P is the vector of points, UB and LB are the upper and lower bound vectors, *rand* creates evenly distributed number in the range [0, 1]. The fitness function of each particle is evaluated to find the Best Point (BP) among all particles.

B. Diffusion Process: Gaussian walk is employed to generate new points in the diffusion stage. The sequence of Gaussian Random Walks (*GRW*) used in diffusion stage are given by:

$$GRW_1 = Gaussian\ (\ |BP|\ ,\ SD) + (rand\ \times\ BP - rand_1\ \times\ P_i) \tag{7}$$

$$GRW_2 = Gaussian\ (|P_i|\ \ ,\ \ SD) \tag{8}$$

Where P_i is the i-th point, *rand* and $rand_1$ are the random numbers as defined above, SD is the standard deviation which is calculated as:

$$SD = \left|\frac{\log(g)}{g} \times (P_i - BP)\right| \tag{9}$$

Where g is the generation number.

C. Updating Process: Every particle is ranked based on their fitness values and each particle i is given a probability value expressed as:

$$P_{pi} = \frac{rank(P_i)}{N} \tag{10}$$

Where P_{pi} is the assigned probability of particle P_i, *rank* (P_i) is the rank of P_i and N is the number particles. The j-th component of P_i is updated if P_{ai}<*rand*, otherwise it remains same. The modified position ofP_i, $P_i^{'}$ is calculated as:

$$P_i^{'} = P_x(j) - rand\ \left[P_y(j) - P_i(j)\right] \tag{11}$$

Where P_x and P_y are arbitrary chosen points in the group.

All the points obtained from the first statistical procedure are ranked again and a probability value is assigned as before. The current position is modified to $P_i^{''}$ if the condition $P_{ai}^{'}$<*rand* is satisfied for a new point $P_i^{'}$, otherwise it remains same. The points are calculated:

$$P_i^{''} = P_i^{'} - rand\left[P_x^{'} - BP\right]\ if\quad rand_g \le 0.5 \tag{12}$$

$$P_i^{''} = P_i^{'} - rand\ \left[P_x^{'} - P_y^{'}\right]\ if\quad rand_g > 0.5 \tag{13}$$

Where $P_x^{'}$ and $P_y^{'}$ are random chosen points found from the initial procedure, and $rand_g$ are random numbers created by the Gaussian approach. The point $P_i^{''}$ replaces$P_i^{'}$, if the fitness value of $P_i^{''}$ is better than $P_i^{'}$.

5.2. Pattern search technique

Pattern search algorithm is an effective but simple technique applicable to the complex problems which cannot be solved by conventional optimization techniques. It has a flexible operator to fine tune the local explore capability. The PS technique involves a series of polls $x_k,\ k \in N$. A trial steps s_k^i with $i = 1, 2, \ldots p$ are added to the polls x_k to get trial points $x_k^i = x_k + s_k^i$ at each poll. At these trial

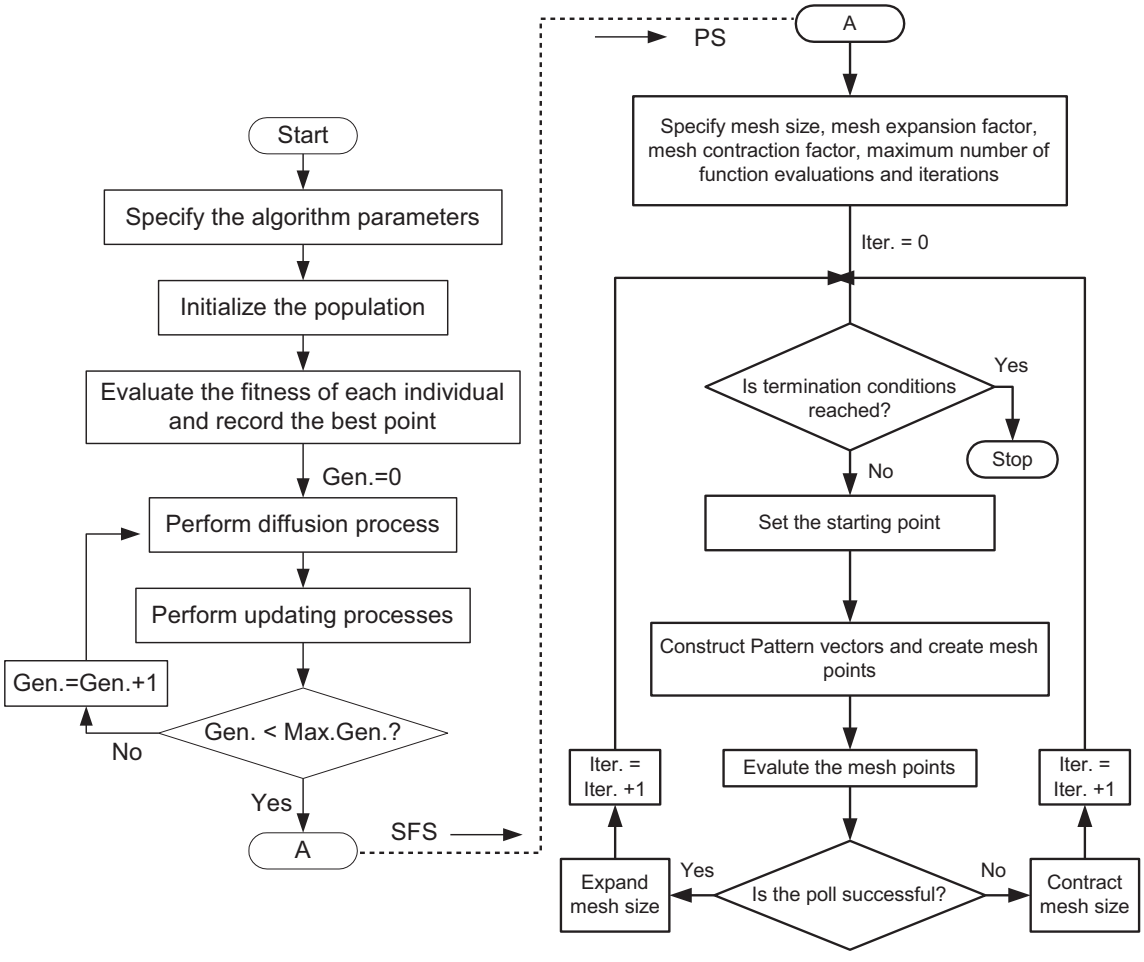

Fig. 5. Flowchart of hSFS-PS algorithm.

Table 1
Integral controller parameters and performance of single area system with various optimization techniques.

Controller parameters/ performance/technique		hSFS-PS	SFS	TLBO [28]	DE [27]	Optimal controller [26]
Parameter value	K_{I1}	0.0418	0.0417	0.0511	0.0516	0.1514
	K_{I2}	0.0144	0.0143	0.0041	0.0071	0.0131
	K_{I3}	0.2146	0.2129	0.1847	0.1701	0.0708
ITAE $\times 10^{-2}$		45.02	45.21	51.35	51.65	99.34
IAE $\times 10^{-2}$		18.96	18.98	19.24	19.54	23.01
ITSE $\times 10^{-3}$		17.32	17.28	17.72	18.2	17.84
ISE $\times 10^{-3}$		8.723	8.742	8.844	8.994	8.3
Settling time (sec)		4.74	4.75	4.89	5.01	8.84

points the objective function value is calculated through a sequence of exploratory steps and compared with its previous value $J(x_k)$. The trial step s_k^* corresponding to least value of $J(x_k + s_k^i) - J(x_k) < 0$ is then chosen to generate the subsequent point $x_{k+1} = x_k + s_k^*$. The trial steps s_k^i are created by a parameter $\Delta_k \in R_+^n$ known as step length parameter. The Δ_k value is modified in subsequent polls as per x_{k+1} value. The improvement of Δ_k, help the algorithm to converge. The detail of PS algorithm has been explained in Ref. [30].

6. Results

6.1. Single area power system

Firstly, a single area power system with integral controllers illustrated in Fig. 1 is considered. The integral controller is initially chosen for better illustration of advantage of proposed optimization technique over some of the recently proposed technique such as Optimal controller [26] DE [27] and TLBO [28]. It is worthwhile to mention that for a fair comparison of optimization techniques, identical system and controller should be used. The integral gains are tuned using ITAE objective function by applying a 1% step load perturbation (SLP) employing SFS algorithm. The ranges of the gains are chosen as (2, −2). For the execution of SFS technique a series of runs were performed to properly choose the algorithm parameters. The following algorithm parameters are used: number of start points (initial populations) = 20, the maximum generations = 20, maximum diffusion = 1. As suggested in literature, 25 independent algorithms are executed and the best values obtained in 25 runs are selected as the integral gains. In the next step, PS is applied to fine tune controller parameter. The final controller parameters found by SFS algorithm are used in PS algorithm as starting points. The PS is implemented with following parameters: mesh size = 1, mesh expansion factor = 2, mesh contraction factor = 0.5, maximum number of objective function evaluations = 50, maximum generations = 10. The flow chart of the hSFS-PS algorithm is shown in Fig. 5. The final solutions for single area power system with integral controller as well as their performance are shown in Table 1 for SFS and hSFS-PS algorithm. For comparison, the corresponding values with TLBO [28], DE [27] and optimal control [26] for the identical system and controller are also given in Table 1. It is obvious from Table 1 that SFS outperforms TLBO [28], DE [27] and optimal control [26] approaches as less ITAE value is found by SFS algorithm (ITAE = 45.21×10^{-2}) compared to TLBO (ITAE = 51.35×10^{-2}), DE (ITAE = 51.65×10^{-2}) and optimal control (ITAE = 99.34×10^{-2}). The ITAE value is further reduced to 45.02×10^{-2} by hSFS-PS algorithm. Consequently, minimum settling time in frequency deviation (5% band) is attained with hSFS-PS compared to other approaches. It is also evident from Table 1 that less IAE, ITSE and ISE values are acquired with proposed hSFS-PS technique compared to other techniques. To further improve the system performance PI, PID and cascade PI-PD controllers are assumed and the parameters are tuned by hSFS-PS algorithm. The results are gathered in Table 2 from which is evident that less ITAE value is got by hSFS-PS optimized cascade PI-PD controller (ITAE = 3.66×10^{-2}) compared to PID (ITAE = 4.45×10^{-2}) and PI (ITAE = 6.07×10^{-2}) controllers. In the next step cascade PI-PD controllers are tuned by proposed hSFS-PS algorithm in presence of PEVs. The optimized parameters are given in Table 2 from which it is evident that ITAE value is decreased to 1.93×10^{-2} by the dynamic support of PEVs during the disturbance.

To examine the time-domain performance, a Step Load Perturbation (SLP) of 1% is considered and system frequency response with proposed hSFS-PS optimized cascade PI-PD controller is provided in Fig. 6 from which it is clear that better system response is obtained with cascade PI-PD controller than conventional PI and PID controller. The system response is significantly improved with

Table 2
Controller parameters and performance of single area system with different controllers.

Controllers parameters/ITAE	With PI controller	With PID controller	With PIPD controller	With EV & PIPD controller
Parameter values	**Unit 1: Thermal**	**Unit 1: Thermal**	**Unit 1: Thermal**	**Unit 1: Thermal**
	$K_{P1} = 1.8283$	$K_{P1} = 1.9663$	$K_{P1T} = 1.7376$	$K_{P1T} = 2.2950$
	$K_{I1} = 0.2290$	$K_{I1} = 0.2206$	$K_{IT} = 1.4439$	$K_{IT} = 2.3992$
		$K_{D1} = 0.9861$	$K_{DT} = 0.8424$	$K_{DT} = 1.2592$
			$K_{P2T} = 1.7822$	$K_{P2T} = 1.9939$
	Unit 2: Hydro	**Unit 2: Hydro**	**Unit 2: Hydro**	**Unit 2: Hydro**
	$K_{P2} = 0.0221$	$K_{P2} = 1.5564$	$K_{P1H} = 1.5093$	$K_{P1H} = 0.5906$
	$K_{I2} = 0.0120$	$K_{I2} = 0.0672$	$K_{IH} = 0.3950$	$K_{IH} = 0.0405$
		$K_{D2} = 0.8125$	$K_{DH} = 0.0919$	$K_{DH} = 1.7872$
			$K_{P2H} = 1.7822$	$K_{P2H} = 1.9939$
	Unit 3: Gas	**Unit 2: Hydro**	**Unit 3: Gas**	**Unit 3: Gas**
	$K_{P3} = 0.4700$	$K_{P3} = 0.5762$	$K_{P1G} = 1.0574$	$K_{P1G} = 0.1177$
	$K_{I3} = 1.0746$	$K_{I3} = 1.6836$	$K_{IG} = 1.6114$	$K_{IG} = 2.3650$
		$K_{D3} = 1.1549$	$K_{DG} = 1.0018$	$K_{DG} = 0.7949$
			$K_{P2G} = 1.7822$	$K_{P2G} = 1.9939$
ITAE $\times 10^{-2}$	6.07	2.71	2.58	2.24

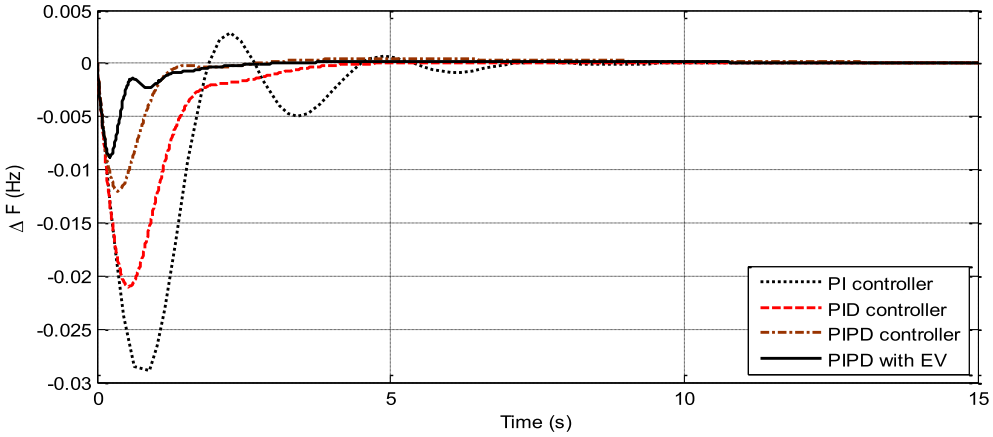

Fig. 6. Frequency deviation of single-area system for 1% SLP with hSFS-PS optimized controllers.

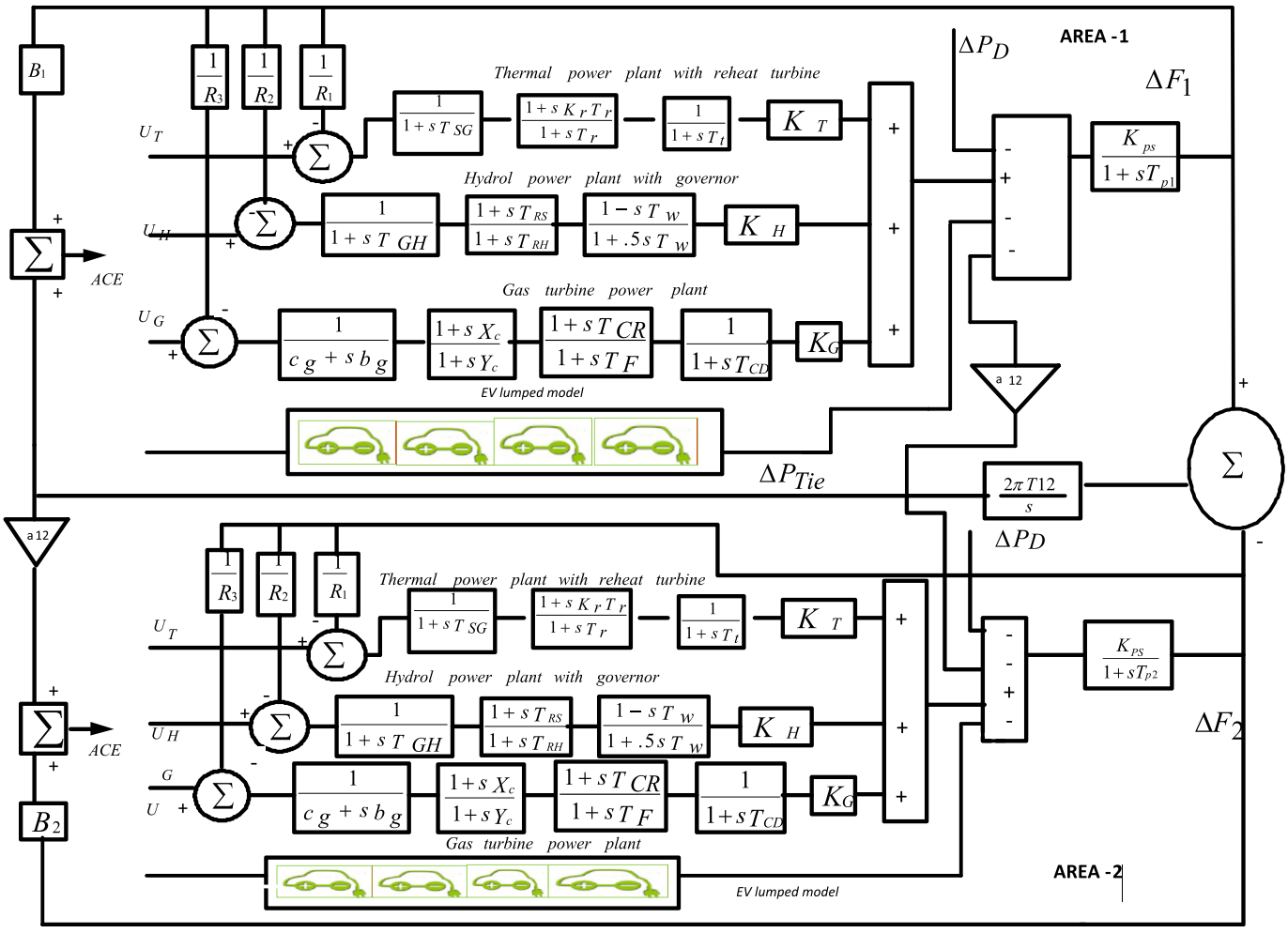

Fig. 7. Two area six unit interconnected power system with PEVs.

the inclusion of PEVs as evident from Fig. 6.

6.2. Extension to 2-area 6-units system

The study is also extended to a multi-area interconnected power system as shown in Fig. 7. The nominal system parameters are provided in Appendix B.

The objective function is modified to include the tie-line power errors and expressed as:

$$J = ITAE = \int_0^{t_{sim}} (|\Delta F_1| + |\Delta F_2| + |\Delta P_{Tie}|) \cdot t.dt \tag{14}$$

Table 3
Various controller parameters and performance of two area system with hSFS-PS optimization technique.

Controller parameters/performance/ technique		PID Controller without EV	PID Controller with EV	PIPD Controller with EV
Parameter values		**Unit 1: Thermal**	**Unit 1: Thermal**	**Unit 1: Thermal**
		$K_{P1} = -1.7074$	$K_{P1} = -1.6062$	$K_{P1T} = 1.2045$
		$K_{I1} = -1.9589$	$K_{I1} = -1.9258$	$K_{IT} = 1.435$
		$K_{D1} = -1.3934$	$K_{D1} = -1.9281$	$K_{DT} = -1.9874$
				$K_{P2T} = -1.8746$
		Unit 2: Hydro	**Unit 2: Hydro**	**Unit 2: Hydro**
		$K_{P2} = -0.7453$	$K_{P2} = -1.6995$	$K_{P1H} = -1.4991$
		$K_{I2} = 0.1375$	$K_{I2} = -0.0148$	$K_{IH} = -1.0789$
		$K_{D2} = -0.9896$	$K_{D2} = 1.0022$	$K_{DH} = -1.1574$
				$K_{P2H} = -0.4478$
		Unit 3: Gas	**Unit 3: Gas**	**Unit 3: Gas**
		$K_{P3} = -1.8253$	$K_{P3} = -0.3612$	$K_{P1G} = 0.331$
		$K_{I3} = -1.6813$	$K_{I3} = -1.7917$	$K_{IG} = -1.9004$
		$K_{D3} = -0.1628$	$K_{D3} = -1.6031$	$K_{DG} = 0.3906$
				$K_{P2G} = 1.917$
ITAE $\times 10^{-2}$		38.18	35.43	19.63
IAE $\times 10^{-2}$		14.71	8.855	6.123
ITSE $\times 10^{-4}$		22.13	8.99	4.847
ISE $\times 10^{-4}$		20.48	9.362	5.415
Settling time in secs	Δf_1	0.49	0.2	0.18
	Δf_2	0.25	0.29	0.27
	ΔP_{Tie}	0.4	0.2800	0.25

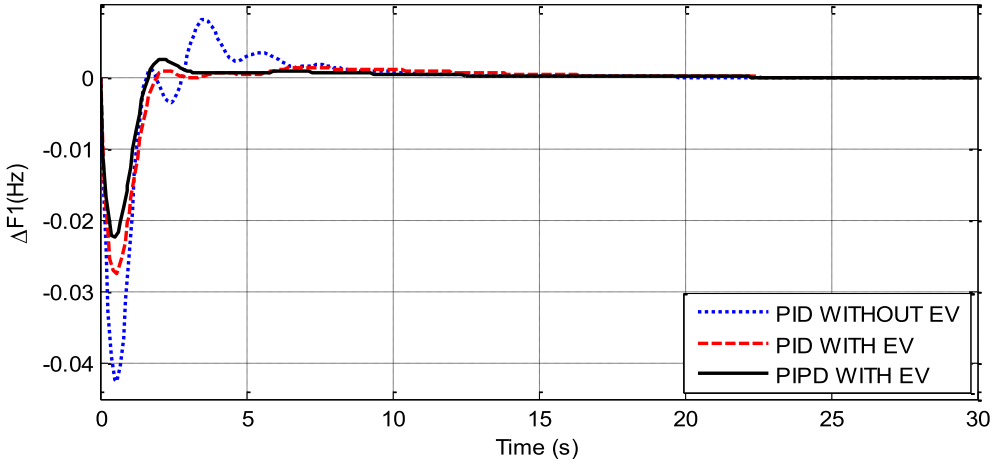

Fig. 8. Frequency deviation of area 1for Two-area system with 2% SLP with hSFS-PS optimized controllers.

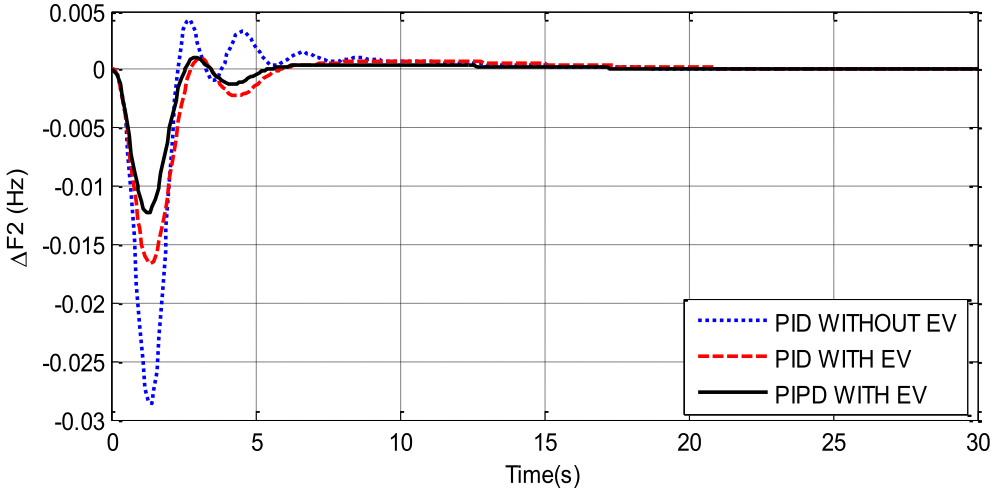

Fig. 9. Frequency deviation of area 2 for Two-area system with 2% SLP with hSFS-PS optimized controllers.

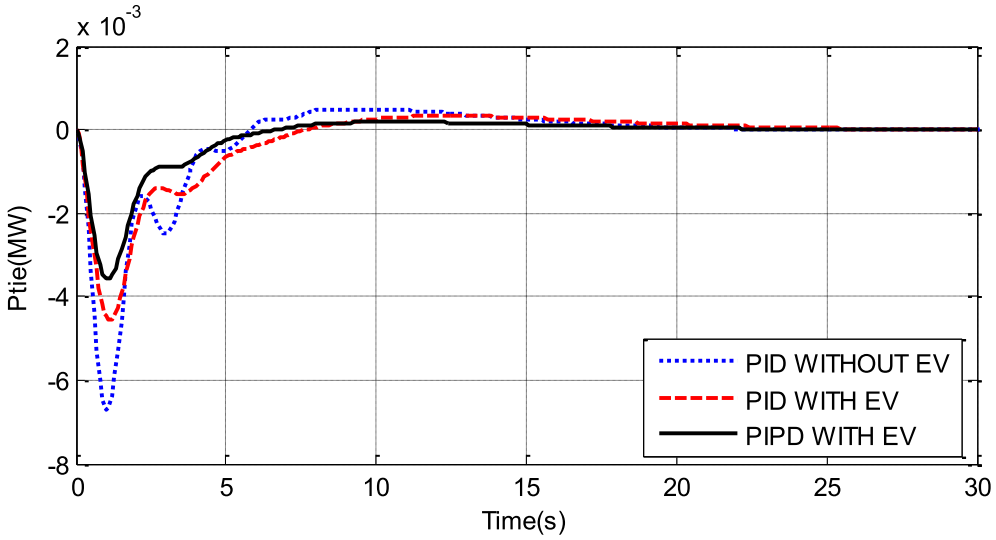

Fig. 10. Tie line power deviation of area 2 for Two-area system with 2% SLP with hSFS-PS optimized controllers.

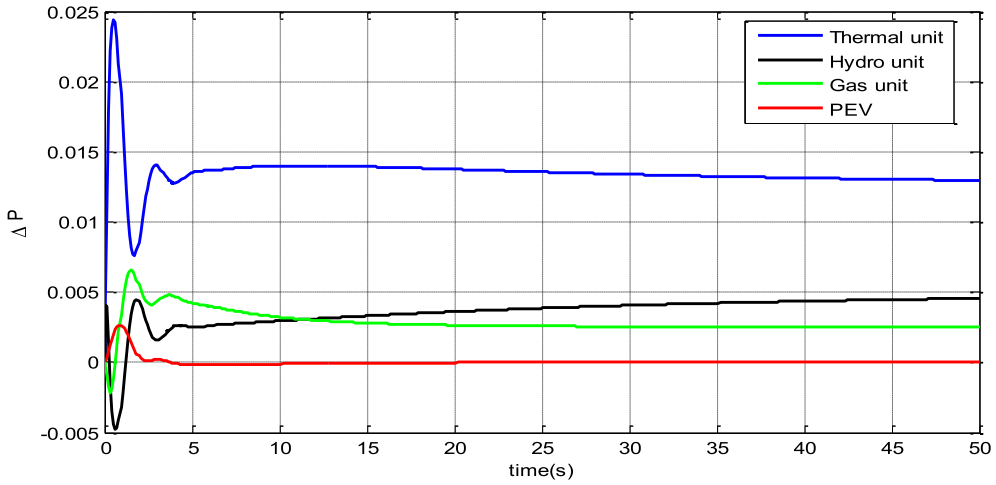

Fig. 11. Variation of power in different units &PEV in 2area-6unit system with 2% step load perturbation.

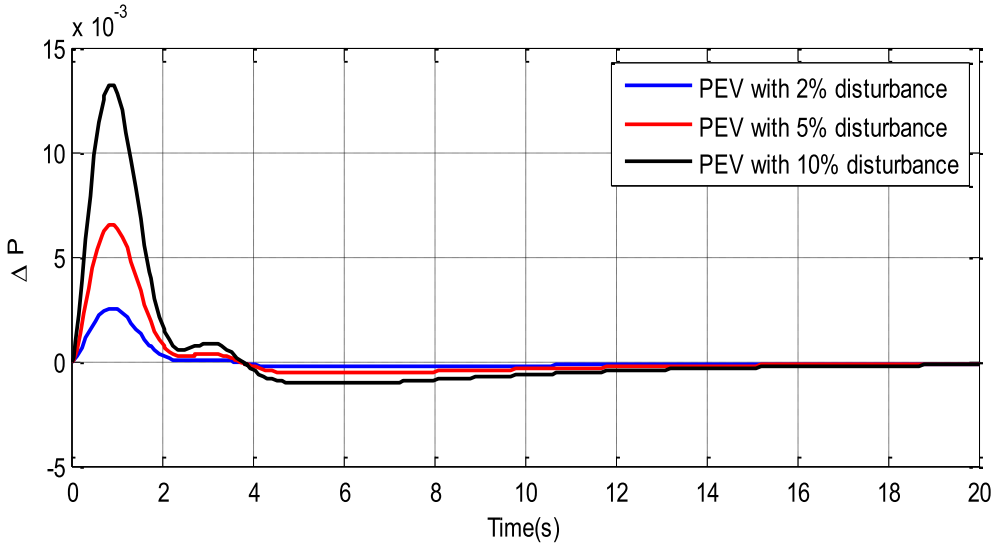

Fig. 12. Power variation of PEV at different disturbances in 2area-6unit system.

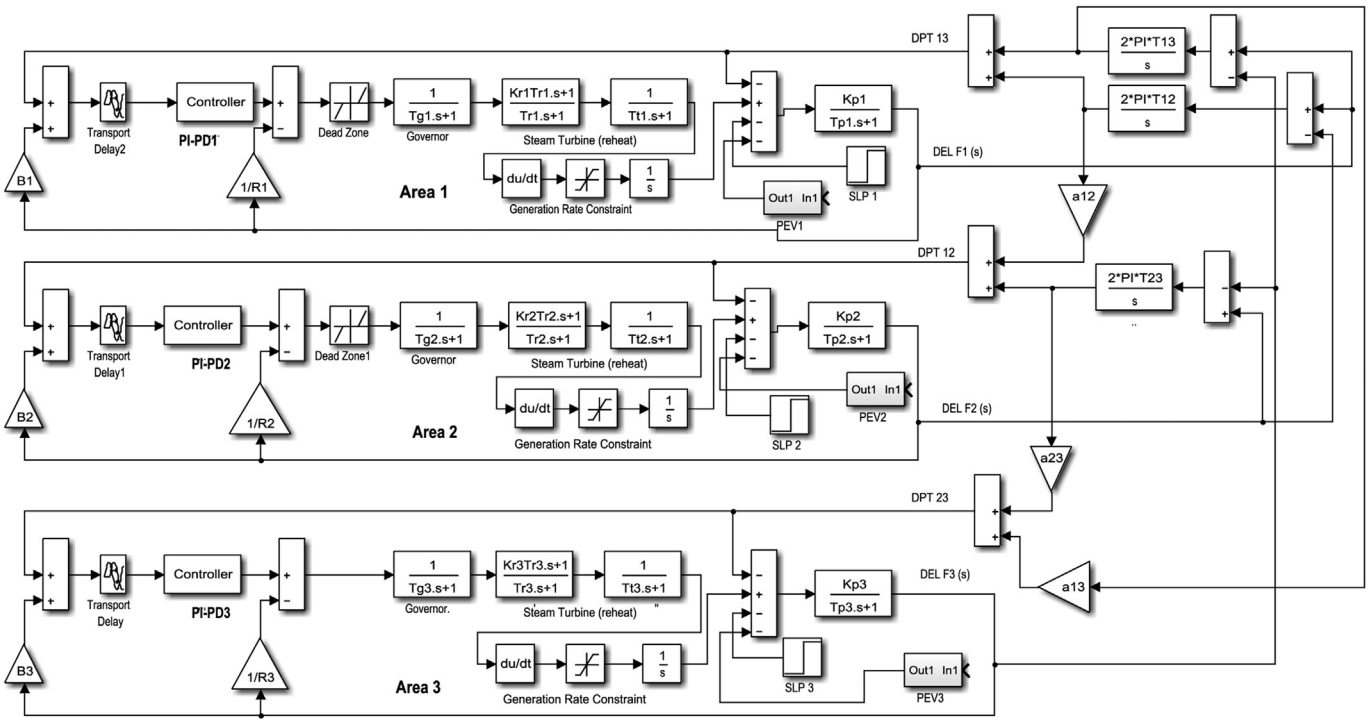

Fig. 13. Three area system with PEV considering GRC, dead band and transport delay.

Table 4
Various controller parameters and performance of three area system with hSFS-PS optimization technique.

Controller parameters/performance/technique	PID Controller with EV	PIPD Controller with EV
Parameter values	**AREA 1: Thermal**	**AREA 1: Thermal**
	$K_{P1} = -1.6756$	$K_{P1} = -0.0568$
	$K_{I1} = 0.1442$	$K_{I1} = 0.4784$
	$K_{D1} = -0.062$	$K_{D1} = -1.9918$
		$K_{P11} = 1.4542$
	AREA 2: Thermal	**AREA 2: Thermal**
	$K_{P2} = -0.3734$	$K_{P2} = 0.7839$
	$K_{I2} = 0.4908$	$K_{I2} = -1.1108$
	$K_{D2} = 0.4878$	$K_{D2} = 0.7807$
		$K_{P22} = -0.5666$
	AREA 3: Hydro	**AREA 3: Hydro**
	$K_{P3} = -0.461$	$K_{P3} = -0.0274$
	$KI_3 = 0.1867$	$K_{I3} = -0.3259$
	$K_{D3} = 0.011$	$K_{D3} = 0.7304$
		$K_{P33} = -1.3726$
ITAE	7.567	1.3524

Where, ΔF_1 and ΔF_2 deviations in frequency of area 1 and area 2; ΔP_{Tie} is the deviation in tie line power; t is the time at any instant and t_{sim} is the simulation time.

Initially, both PID and cascade PI-PD controllers are assumed and the parameters are tuned employing hSFS-PS algorithm as explained earlier. Then PEVs are included in the system and the process is repeated. The optimized controller parameters are provided in Table 3. The various errors and settling times in frequency and tie-line power are also provided in Table 3. It is evident from Table 3 that less ITAE value is obtained with hSFS-PS optimized cascade PI-PD controller (ITAE $= 35.43 \times 10^{-2}$) compared to PID (ITAE $= 38.18 \times 10^{-2}$) and the ITAE value is further reduced to 19.63×10^{-2} when PEVs are included in the system model. It is also clear from Table 3 that minimum IAE, ITSE and ISE values as well as settling times are obtained with cascade PI-PD controller in presence of PEVs compared to individual PID controller and cascade PI-PD controller.

A 2% SLP in area 1 is applied at t = 0 s and the results are shown in Figs. 8–10. It is clear from Figs. 8–10 that better system response is obtained with cascade PI-PD controller than conventional PID controller and the best system response is obtained with the inclusion of PEVs as shown in Figs. 8–10. The variation of powers of different units for the above SLP is illustrated in Fig. 11 from which it is evident that PEVs contribute in the LFC to maintain the system frequency as per the load variations.

To show the contributions made by PEVs, different step load disturbances are applied and power variation of PEVs are shown in Fig. 12. It is evident from Fig. 12 that as the size of load disturbance increases, PEVs contribute more during transient period to improve the system frequency response.

6.3. Extension to three area system with nonlinearities

To prove the capability of the proposed approach to deal with

interconnected power systems which have dissimilar controllers and nonlinearities a three area system [13,35,36] as shown in Fig. 13 is considered. The system comprises thermal and hydro units with PEVs and dissimilar controllers in each area. To get a precise understanding of the AGC problem, it is essential to consider the vital physical constraints. The main physical constraints which have adverse impact on system performance are Generation Rate Constraint (GRC), Governor Dead Band (GDB) nonlinearity and time

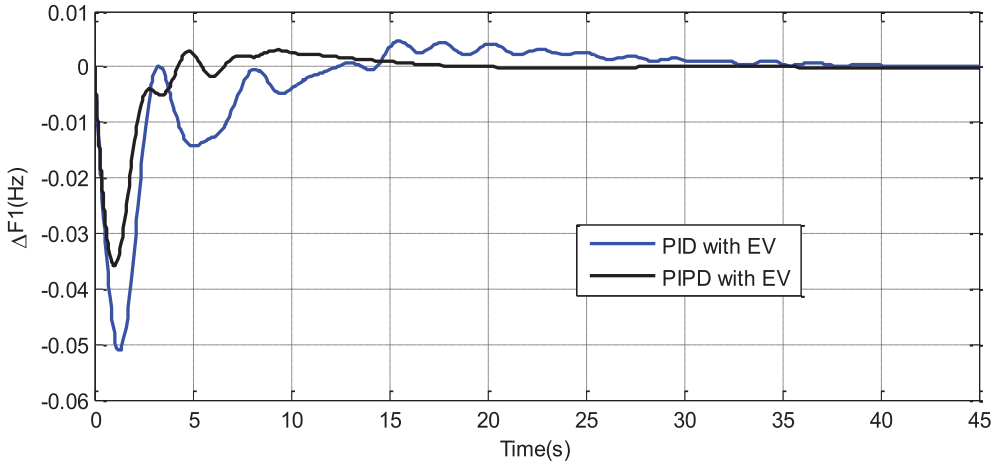

Fig. 14. Frequency change of area 1 with 1% SLP in all areas with hSFS-PS optimized controllers.

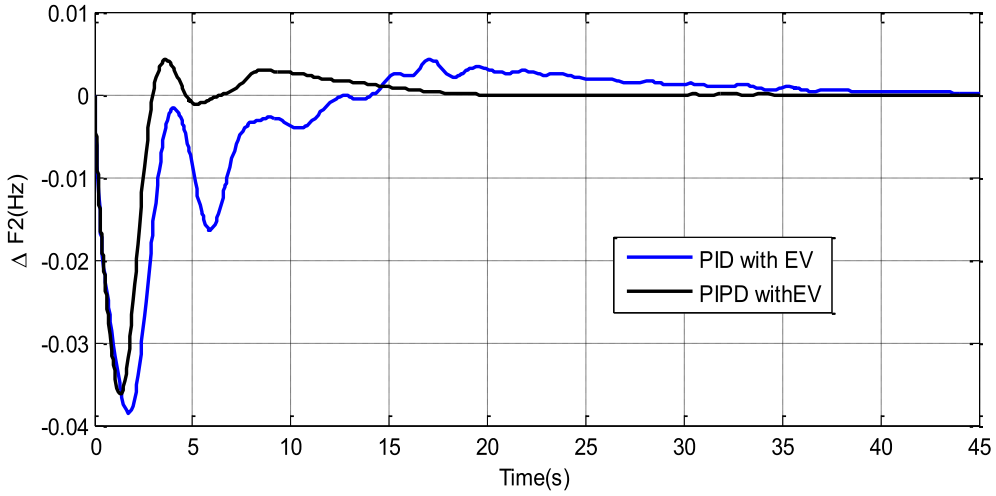

Fig. 15. Frequency change of area 2 with 1% SLP in all areas with hSFS-PS optimized controllers.

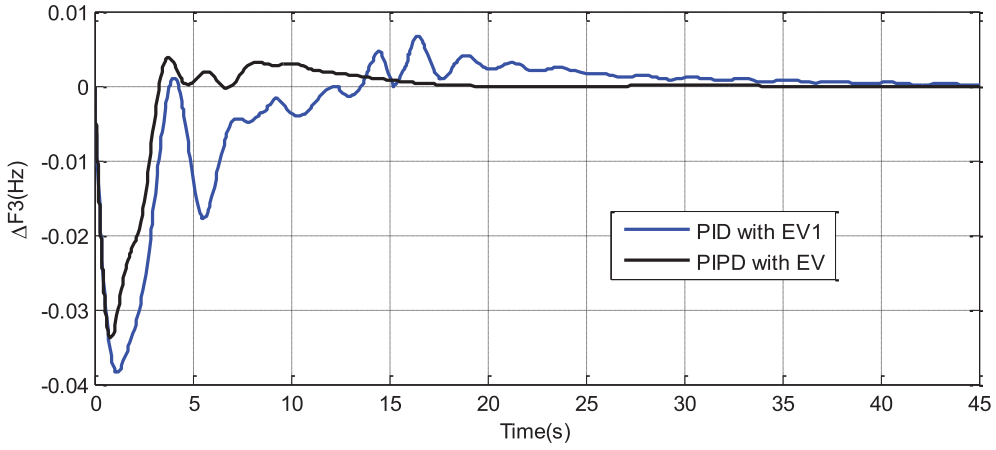

Fig. 16. Frequency change of area 3 with 1% SLP in all areas with hSFS-PS optimized controllers.

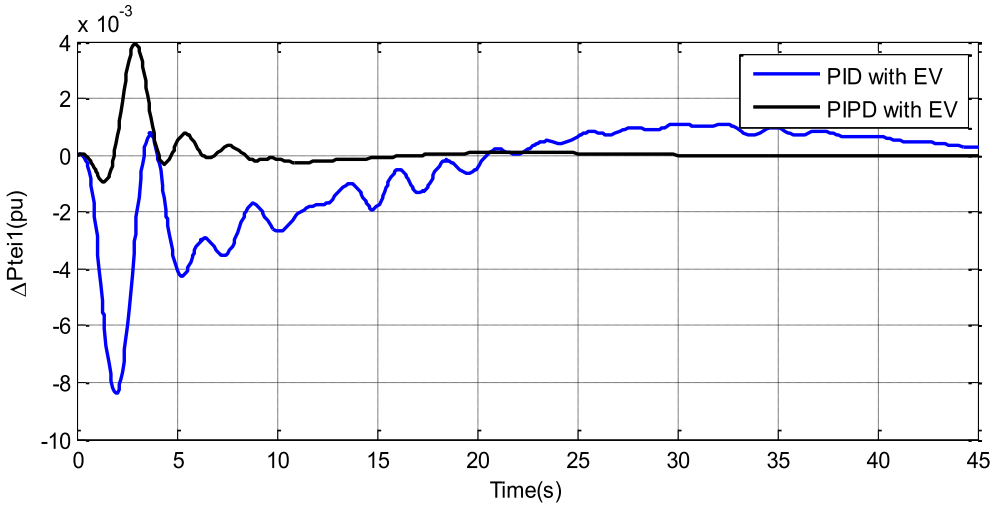

Fig. 17. Tie line power change of Area 1 with 1% SLP in all areas with hSFS-PS optimized controllers.

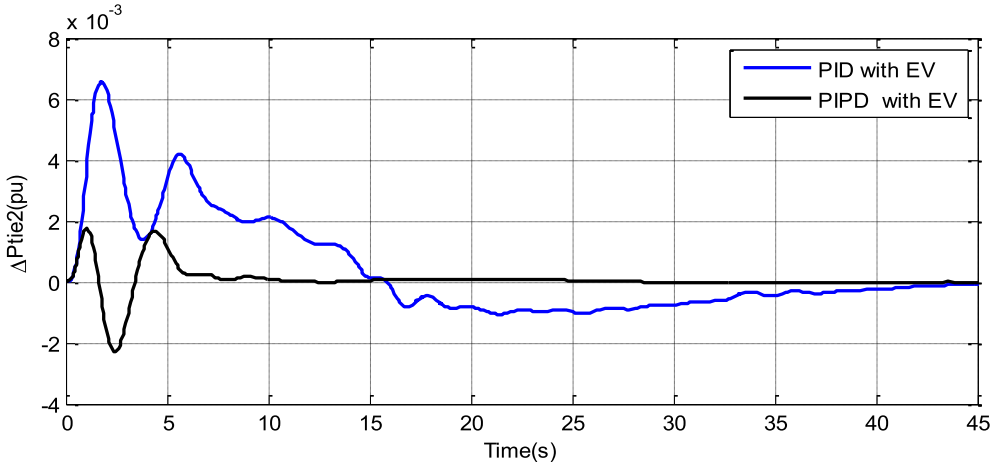

Fig. 18. Tie line power deviation of Area 2 with 1% SLP in all areas with hSFS-PS optimized controllers.

delay. Hence, the effect of GRC, GDB and time delay included in the system model. In a power system having thermal and hydro units, power generation can change only at a definite rate. Typical values of GRCs are: 3–10% p.u. MW/min for thermal [35], 270%/min for raising generation and 360%/min for lowering generation [36] for hydro. The speed governor dead band (GDB) effect rises the

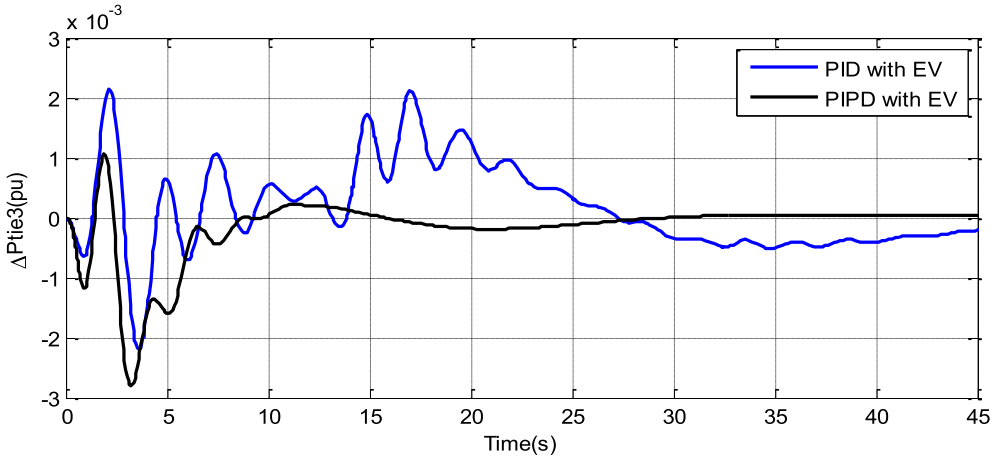

Fig. 19. Tie line power deviation of Area 3 with 1% SLP in all areas with hSFS-PS optimized controllers.

apparent steady-state speed regulation and makes the system oscillatory. In the present study, for thermal units a GRC of 3%/min is assumed. Along with these nonlinearities, a transport delay of 50 ms is introduced between the input and output of controllers in each area. The same procedure as presented earlier is followed to tune the controller parameters. The controller parameters found using hSFS-PS technique and are given in Table 4.

A 1% step load disturbance is applied simultaneously in all the three areas at t = 0 s and the system responses are shown in Figs. 14–19. Critical analysis of the system dynamic responses clearly shows that performance of the system is significantly improved with proposed controller compared to conventional PID controller in presence of PEV.

7. Conclusion

Automatic Generation Control (AGC) of multi-unit systems with diverse power generation sources with plug in electric vehicles is addressed in this study. Firstly, a single area power system with thermal, hydro and gas units is considered and the superiority of SFS algorithm over some recently proposed approaches such as optimal control, DE and TLBO is demonstrated. The local Pattern search technique is then applied to improve the system performance further. Then PEVs are considered and a cascaded PI-PD controller is proposed. The controller parameters are tuned employing proposed hSFS-PS technique. It is demonstrated that best system performance is attained with cascade PI-PD controller in presence of PEVs. The approach is then applied in two area interconnected power system with PEVs in each area. It is found that better system response is obtained with hSFS-PS optimized cascade PI-PD controller in presence of PEVs than some recently proposed approaches like DE and TLBO. Lastly a three area nonlinear power system with PEVs dissimilar controllers is considered. It is seen that proposed hSFS-PS optimized cascade PI-PD controller provides better system response compared to the conventional PID controllers in this case also. It is observed that, in all cases PEVs participate in the LFC to improve the system frequency response.

Appendix A. Single area three unit system & stored energy model of one local center

B = 0.4312 p.u. MW/Hz; P_{rt} = 2000 MW; P_L = 1840 MW; $R_1 = R_2 = R_3$ = 2.4 Hz/p.u.; T_{SG} = 0.08 s; T_T = 0.3s; K_R = 0.3 p.u.; T_R = 10 s; K_{PS} = 68.9566 Hz/p.u. MW; T_{PS} = 11.49 s; T_{12} = 0.0433; $a_{12} = -1$; T_W = 1 s; T_{RS} = 5 s; T_{RH} = 28.75 s; T_{GH} = 0.2 s; X_C = 0.6s; Y_C = 1 s; c_g = 1; b_g = 0.05 s; T_F = 0.23 s; T_{CR} = 0.01s; T_{CD} = 0.2 s; K_T = 0.543478 p.u.; K_H = 0.326084 p.u.; K_G = 0.130438 p.u.;

$N_{contolin}(t) = 12$; $N_{initial}(t) = 90$; $N_{plugout}(t) = 20$; $N_{controllable}(t) = 82$;

Appendix B. Two area six-unit system

$B_1 = B_2$ = 0.4312 p.u. MW/Hz; P_{rt} = 2000 MW; P_L = 1840 MW; $R_1 = R_2 = R_3$ = 2.4 Hz/p.u.; T_{SG} = 0.08 s; T_T = 0.3s; K_R = 0.3 p.u.; T_R = 10 s; $K_{PS1} = K_{PS2}$= 68.9566 Hz/p.u. MW; $T_{PS1} = T_{PS2}$ = 11.49 s; T_{12} = 0.0433; $a_{12} = -1$; T_W = 1 s; T_{RS} = 5 s; T_{RH} = 28.75 s; T_{GH} = 0.2 s; X_C = 0.6s; Y_C = 1 s; c_g = 1; b_g = 0.05 s; T_F = 0.23 s; T_{CR} = 0.01s; T_{CD} = 0.2 s; K_T = 0.543478 p.u.; K_H = 0.326084 p.u.; K_G = 0.130438 p.u.; K_{DC} = 1; T_{DC} = 0.2 s.

Appendix C. Three-area hydro thermal power system with generation rate constraints dead band & transport delay [36]

$B_1 = B_2 = B_3$ = 0.425 p.u. MW/Hz; $R_1 = R_2 = R_3$ = 2.4 Hz/p.u. MW; $T_{G1} = T_{G2}$ = 0.08 s; $T_{r1} = T_{r2}$ = 10.0 s, $T_{T1} = T_{T2}$ = 0.3 s; T_W = 1.0 s; T_R = 5 s;$K_{PS1} = K_{PS2} = K_{PS3}$ = 120 Hz/p.u. MW; $T_{PS1} = T_{PS2} = T_{PS3}$ = 20 s; $T_{12} = T_{23} = T_{31}$ = 0.086 p.u.; $a_{12} = a_{23} = a_{31} = -1$.

References

[1] P. Kundur, Power System Stability and Control, eighth ed., Tata Mc-Graw Hill, New Delhi, 2009.
[2] O.I. Elgerd, Electric Energy Systems Theory: an Introduction, Tata Mc-Graw Hill, New Delhi, 2007.
[3] M. Yilmaz, P.T. Krein, Review of the impact of vehicle-to-grid technologies on distribution systems and utility interfaces, IEEE Trans. Power Electron 28 (12) (2013) 5673–5689.
[4] H. Yang, C.Y. Chung, J. Zhao, Application of plug-in electric vehicles to frequency regulation based on distributed signal acquisition via limited communication, IEEE Trans. Power Syst. 28 (2) (2013) 017–1026.
[5] M. Yilmaz, P.T. Krein, Review of battery charger topologies, charging power levels, and infrastructure for plug-in electric and hybrid vehicles, IEEE Trans. Power Electron 28 (5) (2013) 2151–2169.
[6] C. Guille, G. Gross, A conceptual framework for the vehicle-to-grid (V2G) implementation, Energy Policy 37 (11) (2009) 4379–4390.
[7] H. Liu, Z. Hu, Y. Song, J. Lin, Decentralized vehicle-to-grid control for primary frequency regulation considering charging demands, IEEE Trans. Power Syst. 28 (3) (2013) 3480–3489.
[8] Y. Mu, J. Wu, J. Ekanayake, N. Jenkins, H. Jia, Primary frequency response from electric vehicles in the Great Britain power system, IEEE Trans. Smart Grid 4 (2) (2013) 1142–1150.
[9] Y. Ota, H. Taniguchi, T. Nakajima, K.M. Liyanage, J. Baba, A. Yokoyama, Autonomous distributed V2G (vehicle-to-grid) satisfying scheduled charging, IEEE Trans. Smart Grid 3 (1) (2012) 559–564.
[10] S. Vachirasricirikul, I. Ngamroo, Robust LFC in a smart grid with wind power penetration by coordinated V2G control and frequency controller, IEEE Trans. Smart Grid 5 (1) (2014) 371–380.
[11] H. Liu, Z. Hu, Y. Song, J. Wang, X. Xie, Vehicle-to-grid control for supplementary frequency regulation considering charging demands, IEEE Trans. Power Syst. 30 (6) (2015) 3110–3119.
[12] D.S. Callaway, I.A. Hiskens, Achieving controllability of electric loads, Proc. IEEE 99 (1) (2011) 184–199.
[13] K.R. Sudha, Y.B. Raju, A.C. Sekhar, Fuzzy C-Means clustering for robust decentralized load frequency control of interconnected power system with generation rate constraint, Int. J. Electr. Power Energy Syst. 37 (2012) 58–66.
[14] S.R. Khuntia, S. Panda, Simulation study for automatic generation control of a multi-area power system by ANFIS approach, Appl. Soft Comput. 12 (2012) 333–341.
[15] J.G. Ziegler, N.B. Nichols, Optimum settings for automatic controllers, Trans. ASME 64 (1942) 759–768.
[16] G.H. Cohen, G.A. Coon, Theoretical consideration of retarded control, Trans. ASME 75 (1953) 827–834.
[17] D.E. Rivera, M. Morari, S. Skogestad, Internal model control for PID controller design, Ind. Eng. Chem. Process Des. Dev. 25 (1986) 252–265.
[18] M. Morari, E. Zafiriou, Robust Process Control, Prentice-Hall, Englewood Cliffs NJ, 1989.
[19] W.K. Ho, C.C. Hang, L.S. Cao, Tuning of PID controllers based on gain and phase margin specifications, Automatica 31 (3) (1995) 497–502.
[20] I. Kaya, Obtaining controller parameters for a new PI-PD Smith predictor using auto tuning, J. Process Control 13 (5) (2003) 465–472.
[21] H. Golpira, H. Bevrani, H. Golpira, Application of GA optimization for automatic generation control design in an interconnected power system, Energy Convers. Manag. 52 (2011) 2247–2255.
[22] H. Gozde, M.C. Taplamacioglu, Automatic generation control application with craziness based particle swarm optimization in a thermal power system, Int. J. Electr. Power Energy Syst. 33 (2011) 8–16.
[23] J. Nanda, S. Mishra, L.C. Saikia, Maiden application of bacterial foraging based optimization technique in multiarea automatic generation control, IEEE Trans. Power Syst. 24 (2009) 602–609.
[24] Y.P. Kuo, T.S.S. Li, GA-based fuzzy PI/PD controller for automotive active suspension system, IEEE Trans. Ind. Elect. 46 (6) (1999) 1051–1056.
[25] M. Liu, H. Liu, Q. Sun, T. Zhang, R. Ding, Salient pairwise spatio-temporal interest points for real-time activity recognition, CAAI Trans. Intel. Tech. 1 (1) (2016) 14–29.
[26] K.P.S. Parmar, S. Majhi, D.P. Kothari, Load frequency control of a realistic power system with multi-source power generation, Int. J. Electr. Power Energy Syst. 42 (2012) 426–433.
[27] B. Mohanty, S. Panda, P.K. Hotta, Controller parameters tuning of differential

evolution algorithm and its application to load frequency control of multi-source power system, Int. J. Electr. Power Energy Syst. 54 (2014) 77–85.
[28] A.K. Barisal, Comparative performance analysis of teaching learning based optimization for automatic load frequency control of multi-source power system, Int. J. Electr. Power Energy Syst. 66 (2015) 67–77.
[29] H. Salimi, Stochastic Fractal Search: a powerful metaheuristic algorithm, Knowl. Based Syst. 75 (2015) 1–18.
[30] E.D. Dolan, R.M. Lewis, V. Torczon, On the local convergence of pattern search, SIAM J. Optim. 14 (2003) 567–583.
[31] S. Koichiro, M. Taisuke, O. Yutaka, Y. Akihiko, A new load frequency control method in power system using vehicle-to-grid system considering users' convenience, in: Proceedings of the 17th Power Systems Computation Conference, Stockholm Sweden, August 22-26, 2011.
[32] Y. Lee, S. Park, PID controller tuning to obtain desired closed loop responses for cascade control systems, Ind. Eng. Chem. 37 (1998) 1859–1865.
[33] M.A. Johnson, M.H. Moradi, PID Control: New Identification and Design Methods, Springer International Edition, 2010, pp. 103–106.
[34] P. Dash, L.C. Saikia, N. Sinha, Flower pollination algorithm optimized PI-PD cascade controller in automatic generation control of a multi-area power system, Int. J. Electr. Power Energy Syst. 82 (2016) 19–28.
[35] S. Panda, B. Mohanty, P.K. Hota, Hybrid BFOA-PSO algorithm for automatic generation control of linear and nonlinear interconnected power systems, Appl. Soft Comput. 13 (12) (2013) 4718–4730.
[36] R.K. Sahu, S. Panda, G.T. ChandraSekhar, A novel hybrid PSO-PS optimized fuzzy PI controller for AGC in multi area interconnected power systems, Int. J. Electr. Power Energy Syst. 64 (2015) 880–893.

Sasmita Padhy was born on 29th June 1980 at Ganjam Odisha, India. She obtained her B.Engg (Electrical & Electronics) from National Institute of Science and Technology (NIST) Berhampur Odisha in 2003 and M.Tech (Power System) from BPUT in 2011. Currently She is pursuing Ph.D in VSSUT, Burla and her research interest lies in Power system stability, control and computational intelligence.

Sidhartha Panda is working as a Professor in the Department of Electrical Engineering, Veer Surendrai Sai University of Technology (VSSUT), Burla, Sambalpur, Odisha, India. He received Ph.D. degree from Indian Institute of Technology (IIT), Roorkee, India, M.E. degree from Veer Surendrai Sai University of Technology (VSSUT). His areas of research include Flexible AC Transmission Systems (FACTS), Power System Stability, Soft computing, Model Order Reduction, Distributed Generation and Wind Energy. Dr. Panda is a Fellow of Institution of Engineers (India).